RAY-OPTICS ANALYSIS OF SINGLE MODE CONDITION FOR OPTICAL WAVEGUIDES WITH RECTANGULAR CROSS-SECTION

Xinjie Song[*] and Rainer Leonhardt

Department of Physics, University of Auckland, 38 Princes St., Auckland 1010, New Zealand

Abstract—The single mode condition of rectangular waveguides is derived by using a simple ray-optics approach, which relies on geometrical ray tracing principles as in classical optics. Light propagation through such a waveguide can be approximately simplified as reflections within two planes of incidence. By employing the mode equations for different polarizations, a relation that shows the single-mode cut-off as a function of the waveguide dimensions is readily obtained.

1. INTRODUCTION

Optical waveguides with a wide variety of shapes have been studied during the past decades [1–16]. As one of the most basic structures among them, rectangular waveguides undoubtedly attracted the attention of early researchers. An analytical solution for the modal dispersion problem in a rectangular core guiding structure was first given by Marcatili [2] as early as 1969. He solved Maxwell's equations mathematically by way of separation of variables. In the same year, Goell [17] presented his circular harmonic computer analysis. Other approaches such as Knox and Toulios' [18] equivalent-index method, Yeh's [19] finite-element method, and Jain's [20] variational method have appeared later to solve the problem in different ways. However, all these techniques above analyze modes by a physical-optics method, which involves complex algebraic or differential calculation but does not give an explicit solution for the single mode condition of rectangular dielectric waveguides. The purpose of this paper is to present a convenient ray-optics method to determine the single mode condition

for rectangular waveguides. The analytical solution in this paper is extended from the ray-optics theory of planner waveguide, and optical modes are therefore described in a more visualized and less complicated way. We are using the same approximation as Marcatili, which turns out to be very good for all the cases we looked at. We finally give the theoretical cut-off dimension curves for specific single mode waveguides, and compare our results with computer simulations obtained with a fully-vectorial mode solver.

2. THEORY

As an introduction, we will look at the 2-D waveguide first before we discuss the 3-D waveguide. A particular ray pattern within a slab waveguide is depicted in Fig. 1. According to the ray-optics theory based on classical optics, if light undergoes a constructive interference when propagates through a slab waveguide, the total phase change for a guided wave that bounces once between the two interfaces must be a multiple of 2π [21], expressed as

$$2k_0 n_1 d \sin\theta - 2\varphi_{12} - 2\varphi_{13} = 2m\pi, \quad m = 0, 1, 2, \ldots \quad (1)$$

where m is the mode number, φ_{12} and φ_{13} are the phase changes suffered upon the total internal reflection at the interfaces. Values for the two polarizations are:

$$\begin{cases} \text{TE modes: } \tan\varphi_{12} = \sqrt{\dfrac{1 - \left(\frac{n_2}{n_1}\right)^2}{\sin^2\theta} - 1} & (2) \\[4ex] \text{TM modes: } \tan\varphi_{12} = \left(\dfrac{n_1}{n_2}\right)^2 \sqrt{\dfrac{1 - \left(\frac{n_2}{n_1}\right)^2}{\sin^2\theta} - 1} & (3) \end{cases}$$
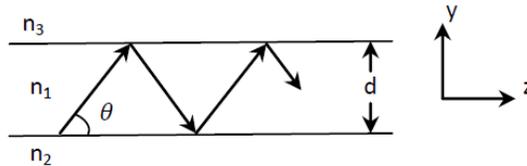
Figure 1. Optical ray pattern within a planar waveguide: n_1, n_2, n_3 are the refractive indices of the core, substrate and cladding, d is the thickness of the core region, θ is the angle of reflection with respect to the z direction.

Each allowed mode has a corresponding effective index, defined as

$$n_{eff} = n_1 \cos\theta \tag{4}$$

Only when $n_2 \leq n_{eff} \leq n_1$, mode is well confined in the core region. So for a slab waveguide, the critical condition of guided modes would be (assuming $n_2 \geq n_3$)

$$n_{eff} = n_2 \tag{5}$$

Now let us consider the light propagation in a 3-D rectangular waveguide. The basic configuration to be studied is shown in Fig. 2. Accordingly, light within such a core guiding structure can be characterized by values of (θ, α) [Fig. 3(a)]. A ray propagating in a spiral-like fashion can therefore be decomposed to be two zig-zag paths within different planes of incidence.

Figure 3(a) shows the reflection at the top- and bottom interfaces. AO is the actual ray, with a unique set of values for (θ, α). $(\frac{\pi}{2} - \theta)$ indicates the incident angle within the incident plane AOC, α is the angle between plane AOC and z direction (BO). Fig. 3(b) illustrates the reflection between the left- and right interfaces. $(\frac{\pi}{2} - \theta')$ indicates the incident angle within the incident plane AOD. Accordingly, the effective index is defined as

$$n_{eff} = n_1 \cos\theta \cos\alpha \tag{6}$$

As shown in Fig. 2, the two angles of incidence have a relation as

$$\sin\theta' = \frac{AD}{OA} = \frac{BC}{OA} = \frac{OC \cdot \sin\alpha}{OC/\cos\theta} = \sin\alpha \cdot \cos\theta \tag{7}$$

From Eq. (1), the constructive interference conditions at the horizontal and vertical boundaries result in:
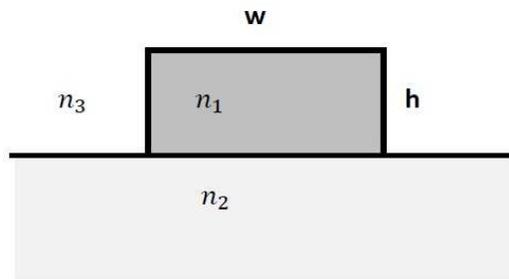
Figure 2. Cross section for a typical rectangular waveguide: w, h are the width and height of the core region.

$$\begin{cases} k_0 n_1 h \sin\theta = m\pi + \varphi_{12} + \varphi_{13}, & m = 0, 1, 2, \dots \quad (8) \\ k_0 n_1 w \sin\theta' = n\pi + 2\varphi_{13}, & n = 0, 1, 2, \dots \quad (9) \end{cases}$$

Next we will consider the propagation characteristics of the modes. While there is a clear definition of TE and TM modes for 2-D waveguides, for 3-D rectangular waveguides, a definition of E_{pq}^x, E_{pq}^y modes is more useful. In rectangular waveguides, two families of optical modes, noted as E_{pq}^x and E_{pq}^y modes, are strongly polarized along the x and y direction, respectively [22]. The E_{pq}^x modes (p, $q = 1, 2, 3\dots$; p and q denote the number of antinodes of the electric field in the x and y direction, respectively), where the electric field is polarized mainly along the x direction, are equivalent to TE modes in Fig. 3(a) and TM modes in Fig. 3(b). According to Eqs. (2), (3), (8), (9), E_{pq}^x (also noted as $E_{m+1,n+1}^x$, m, $n = 0, 1, 2\dots$) mode can be expressed as:

$$\begin{cases} k_0 n_1 h \sin\theta = m\pi + \tan^{-1}\sqrt{\dfrac{1 - \left(\frac{n_2}{n_1}\right)^2}{\sin^2\theta} - 1} + \tan^{-1}\sqrt{\dfrac{1 - \left(\frac{n_3}{n_1}\right)^2}{\sin^2\theta} - 1} \quad (10) \\[2em] k_0 n_1 w \sin\theta' = n\pi + 2\tan^{-1}\left[\left(\dfrac{n_1}{n_3}\right)^2\sqrt{\dfrac{1 - \left(\frac{n_3}{n_1}\right)^2}{\sin^2\theta'} - 1}\right] \quad (11) \end{cases}$$
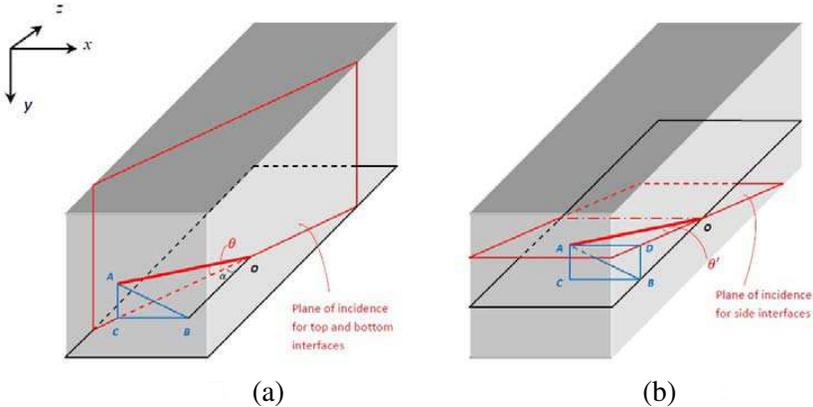
Figure 3. Ray pattern in a rectangular waveguide. (a) Reflection between the horizontal boundaries. (b) Reflection between the vertical boundaries.

Similarly, E_{pq}^y modes, for which the dominant electric field is along the y direction, can be taken as TM modes in Fig. 3(a) and TE modes in Fig. 3(b). Therefore we get:

$$
\begin{cases}
k_0 n_1 h \sin\theta = m\pi + \tan^{-1}\left[\left(\dfrac{n_1}{n_2}\right)^2\sqrt{\dfrac{1-\left(\frac{n_2}{n_1}\right)^2}{\sin^2\theta}-1}\right] \\[6ex]
\qquad\quad + \tan^{-1}\left[\left(\dfrac{n_1}{n_3}\right)^2\sqrt{\dfrac{1-\left(\frac{n_3}{n_1}\right)^2}{\sin^2\theta}-1}\right] \qquad (12) \\[6ex]
k_0 n_1 w \sin\theta' = n\pi + 2\tan^{-1}\sqrt{\dfrac{1-\left(\frac{n_3}{n_1}\right)^2}{\sin^2\theta'}-1} \qquad\qquad (13)
\end{cases}
$$

We thus get the mode Eqs. (10), (11), (12), (13), with which the problem of the single mode condition can be solved. It should also be mentioned that the single mode condition is the same as the cut-off of the first higher order modes — E_{21}^x, E_{12}^x, E_{21}^y and E_{12}^y, so once these modes meet the critical condition (assuming $n_2 > n_3$)

$$ n_{eff} = n_2, \qquad (14) $$

they cannot be supported by the waveguide anymore. It should be noted that Eq. (14) is obtained by extending from the 2-D waveguide case (Eq. (5)). To be specific, when we have a mode that has a n_{eff} which is approaching the refractive indices of the surrounding materials (here we have $n_2 > n_3$, so we use n_2) it is equivalent to having no dielectric boundary, and therefore there is no confinement for the mode.

Take the cut-off condition of E_{21}^x mode for example, substituting $m = 1$ into Eq. (10) we can obtain θ from a given value of height (h), then the angle θ' can be calculated from Eqs. (6), (14), (7), finally we take θ' and $n = 0$ into Eq. (11) to get the corresponding width (w). That is how we plot a curve for the cutoff dimension of the E_{21}^x mode. Cutoff conditions of E_{12}^x, E_{21}^y and E_{12}^y can be worked out in the same manner.

3. RESULTS AND DISCUSSION

Theoretical results of single mode conditions for polymer and silicon waveguides with rectangular cross-section are plotted together with computer simulations obtained with the vectorial mode solver MODE from Lumerical Solutions Inc. [23] in Fig. 4. The regions above the
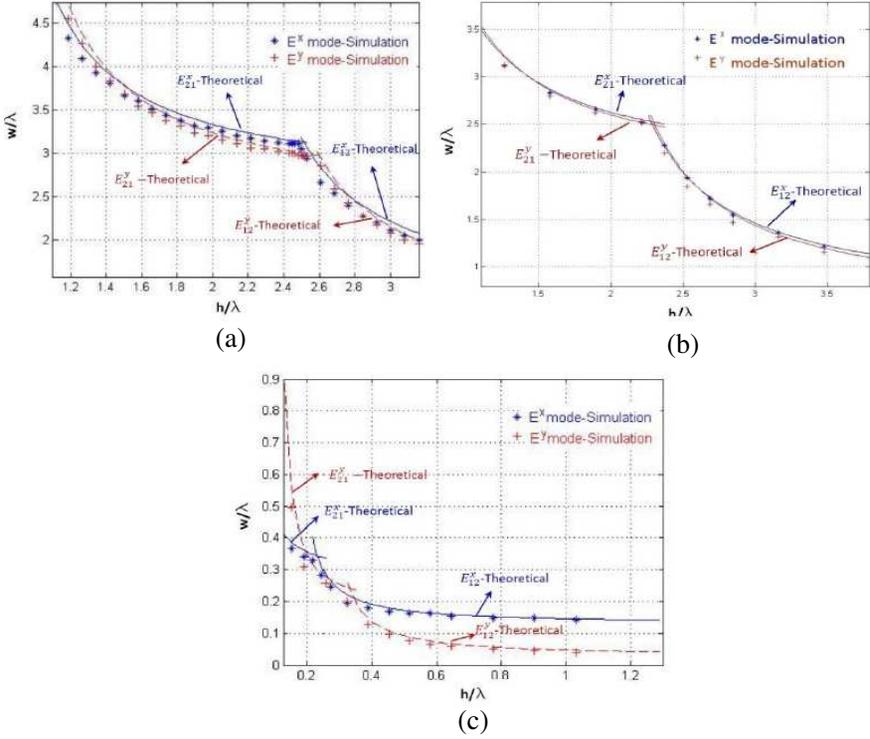
Figure 4. Single mode conditions for (a) Amorphous Polycarbonate (APC) waveguide on glass substrate: $n_1 = 1.558$, $n_2 = 1.5188$, $n_3 = 1$; (b) APC waveguide on glass substrate with Poly (methyl methacrylate) (PMMA) cladding: $n_1 = 1.558$, $n_2 = 1.5188$, $n_3 = 1.49$; (c) Si waveguide on SiO$_2$ substrate: $n_1 = 3.48$, $n_2 = 1.44$, $n_3 = 1$. The curves represent the analytical calculation, the points are the simulation results. (The regions below the curves/points define the parameters for single-mode propagation).

curves/points give the dimensions that are able to guide the first higher order modes. The regions beneath the curves/points indicate dimensions that support single mode propagation.

It should be noted that this ray-optics approach is based on the approximation that the mode is confined to the core region (with evanescent field in areas with n_2, n_3, n_4 and n_5 in Fig. 5), completely ignoring the four corner areas (shaded area in Fig. 5), which are taken into account in physical optics. In practice, this is the main difference between the ray and the fully-vectorial methods. Fig. 4
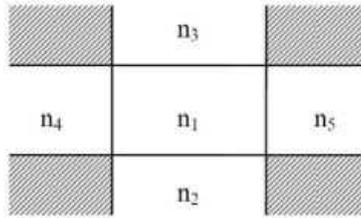
Figure 5. Rectangular waveguide geometry for a general analysis.

shows a very good agreement between the theoretical and simulated results, indicating the validity of our approximation. So when very high precision is not required, the ray-optics approach is a much more convenient method to determine the waveguide dimensions for single mode operation. Especially, from the equations above, we can quickly obtain the theoretical curve, while the simulations only deal with a very limited number of points. Taking Fig. 4(a)) as an example, the theoretical data take only 30 seconds to generate, however, for the simulated points, it takes 3 days of computing time using a standard desktop computer. By studying the mode equations, it is mathematically proven that greater n_2 and smaller n_3 values lead to larger single mode cut-off dimensions, which are desirable for the convenience of manufacturing in most of the cases.

While in this paper only the more common structures of rectangular waveguides have been used to clarify the ray method, for the general case [Fig. 5], in which we have different values for n_3, n_4, n_5, the ray method in a slightly modified version will be valid as well.

4. CONCLUSION

In this paper, we have demonstrated that ray-optics approach is applicable to calculate the single mode conditions of rectangular waveguides much faster than can be done with the physical-optics methods. It also provides a visualized-oriented method to understand the light propagation through 3D waveguides, and the necessary approximation still leads to results that are in very good agreement with our fully-vectorial computer simulations.

REFERENCES

1. Yeh, C., "Elliptical dielectric waveguide," *J. Appl. Phys.*, Vol. 33, 3235–3242, 1962.

2. Marcatili, E. A. J., "Dielectric rectangular waveguide and directional coupler for integrated optics," *Bell Syst. Tech. J.*, Vol. 48, 2071–2102, 1969.

3. James, J. R. and I. N. L. Gallett, "Modal analysis of triangular cored fibre waveguide," *Proc. IEEE*, Vol. 120, 1362–1370, 1973.

4. Gallawa, R. L., I. C. Goyal, Y. Tu, and A. K. Ghatak, "Optical waveguide modes: An approximate solution using Galerkin's method with Hermite-Gauss basis functions," *J. IEEE Quantum Electronics*, Vol. 27, 518–522, 1991.

5. Singh, V., B. Prasad, and S. P. Ojha, "Theoretical analysis and dispersion curves of an annular light guide with a cross-section bounded by two piet-hein curves," *Journal of Electromagnetic Waves and Applications*, Vol. 17, No. 7, 1025–1036, 2003.

6. Shu, H. and M. Bass, "Calculating the guided modes in optical fibers and waveguides," *J. Lightwave Technology*, Vol. 25, 2693–2699, 2007.

7. Pandey, P. C., A. Mishra, and S. P. Ojha, "Modal dispersion characteristics of a single mode dielectric optical waveguide with a guiding region cross-section bounded by two involuted spirals," *Progress In Electromagnetic Research*, Vol. 73, 1–13, 2007.

8. Robinson, J. T. and M. Lipson, "Direction-dependent optical modes in nanoscale silicon waveguides," *Optics Express*, Vol. 19, 18380–18392, 2011.

9. Dong, J., J. Li, and F.-Q. Yang, "Guided modes in the four-layer slab waveguide containing chiral nihility core," *Progress In Electromagnetic Research*, Vol. 112, 241–255, 2011.

10. Dong, J. and J. Li, "Characteristics of guided modes in uniaxial chiral circular waveguides," *Progress In Electromagnetic Research*, Vol. 124, 331–345, 2012.

11. Polky, J. N. and G. L. Mitchell, "Metal-clad planner dielectric waveguide for integrated optics," *J. Opt. Soc. Am.*, Vol. 64, 274–279, 1974.

12. Rickman, A. G., G. T. Reed, and F. Namavar, "Silicon-on-insulator optical rib waveguide loss and mode characteristics," *J. Lightwave Tech.*, Vol. 12, 1771–1776, 1994.

13. Dillon, B. M. and A. A. P. Gibson, "Triply-ridged circular waveguides," *Journal of Electromagnetic Waves and Applications*, Vol. 9, Nos. 1–2, 145–156, 1995.

14. Kesari, V. and J. P. Kesari, "Analysis of a circular waveguide loaded with dielectric and metal discs," *Progress In Electromagnetic Research*, Vol. 111, 253–269, 2011.

15. Tretyakov, O. A. and M. Kaya, "The real-valued time-domain TE-modes in lossy waveguides," *Progress In Electromagnetic Research*, Vol. 127, 405–426, 2012.

16. Fotyga, G., K. Nyka, and M. Mrozowski, "Efficient model order reduction for FEM analysis of waveguide structures and resonators," *Progress In Electromagnetic Research*, Vol. 127, 277–295, 2012.

17. Goell, J. E., "A circular harmonic computer analysis of rectangular dielectric waveguide," *Bell Syst. Tech. J.*, Vol. 48, 2311–2160, 1969.

18. Knox, R. M. and P. P. Toulios, "Integrated circuit for the millimeter through optical frequency range," *Proceedings of MRI Symposium on Submillimeter Waves*, J. Fox, Ed., Polytechnic Press, Brooklyn, 1970.

19. Yeh, C., H. Ha, S. B. Dong, and W. P. Brown, "Single mode optical waveguides," *Appl. Opt.*, Vol. 10, 1490–1504, 1979.

20. Jain, U., A. Sharma, K. Thyagarajian, and A. K. Ghatak, "Coupling characteristics of a diffused channel waveguide directional coupler," *J. Opt. Soc. Am.*, Vol. 72, 1545–1549, 1982.

21. Hunsperger, R. G., *Integrated Optics Theory and Technology*, 6th Edition, Springer, 2009.

22. Lifante, G., *Integrated Photonics: Fundamentals*, Wiley, New Jersey, 2003.

23. Mode Solutions: www.lumerical.com.